

1 **Modelling interactions of acid-base balance and respiratory status**
2 **in the toxicity of metal mixtures in the American oyster *Crassostrea virginica***

3
4 Brett M. Macey^{a,b,h}, Matthew J. Jenny^g, Heidi R. Williams^{a,b}, Lindy K. Thibodeaux^{a,b}, Marion
5 Beal^{a,c}, Jonas S. Almeida^d, Charles Cunningham^{a,d,f}, Annalaura Mancia^{a,d}, Gregory W. Warr^{a,d,i},
6 Erin J. Burge^{a,b,e}, A. Fred Holland^a, Paul S. Gross^{a,d}, Sonomi Hikima^{a,d}, Karen G. Burnett^{a,b}, and
7 Louis Burnett^{a,b}, Robert W. Chapman^{a,b, c,d*}

8
9 ^aHollings Marine Laboratory (HML), Charleston, SC 29412, USA; ^bGrice Marine Laboratory,
10 College of Charleston, Charleston, SC 29412, USA; ^cMarine Resources Research Institute, South
11 Carolina Department of Natural Resources, Charleston, SC 29412, USA; ^dMedical University of
12 South Carolina, Charleston, SC 29425, USA

13 Current affiliations: ^eDepartment of Marine Science, Coastal Carolina University, Conway, SC
14 29526, USA; ^fDepartment of Biology, University of New Mexico, Albuquerque, NM 87131,
15 USA; ^gWoods Hole Oceanographic Institution, Woods Hole, MA 02543, USA; ^hDepartment of
16 Environmental Affairs and Tourism, Marine and Coastal Management, Roggebaai 8012, RSA,
17 ⁱDivision of Molecular and Cellular Biosciences, National Science Foundation, Arlington VA
18 22230.

19
20
21 *Corresponding author: Hollings Marine Laboratory, 331 Fort Johnson Road, Charleston, South
22 Carolina 29412; phone: (843)762-8860; fax: (843)762-8737; e-mail: chapmanr@dnr.sc.gov
23

24 **Abbreviations:** ANN: artificial neural network; LPx: lipid peroxidation; TBARS: thiobarbituric
25 acid-reactive substances; ROS: reactive oxygen species; THC: total hemocyte count; GSH:
26 glutathione; TSA: tryptic soy agar; TCBS: thiosulfatecitrate-bile-sucrose; GLM: general linear
27 models
28

29

30 **Abstract**

31 Heavy metals, such as copper, zinc and cadmium, represent some of the most common and
32 serious pollutants in coastal estuaries. In the present study, we used a combination of linear and
33 artificial neural network (ANN) modelling to detect and explore interactions among low-dose
34 mixtures of these heavy metals and their impacts on fundamental physiological processes in
35 tissues of the Eastern oyster, *Crassostrea virginica*. Animals were exposed to Cd (0.001 – 0.400
36 μM), Zn (0.001 – 3.059 μM) or Cu (0.002 – 0.787 μM), either alone or in combination for 1 to
37 27 days. We measured indicators of acid-base balance (hemolymph pH and total CO_2), gas
38 exchange (PO_2), immunocompetence (total hemocyte counts, numbers of invasive bacteria),
39 antioxidant status (glutathione, GSH), oxidative damage (lipid peroxidation; LPx), and metal
40 accumulation in the gill and the hepatopancreas. Linear analysis showed that oxidative
41 membrane damage from tissue accumulation of environmental metals was correlated with
42 impaired acid-base balance in oysters. ANN analysis revealed interactions of metals with
43 hemolymph acid-base chemistry in predicting oxidative damage that were not evident from
44 linear analyses. These results highlight the usefulness of machine learning approaches, such as
45 ANNs, for improving our ability to recognize and understand the effects of sub-acute exposure to
46 contaminant mixtures.

47

48 **Keywords:** heavy metals, artificial neural networks, *Crassostrea virginica*, lipid peroxidation,
49 glutathione, acid-base balance, hemolymph PO_2

50

51 **1. Introduction**

52

53 Industrialization and urbanization along the coastline of the US have substantially increased
54 the amount and variety of anthropogenic pollutants entering estuarine ecosystems. Among the
55 most common of these contaminants, heavy metals are of particular concern because they persist
56 in the environment and have a wide variety of adverse effects. Developing biomarkers and
57 predicting effects of contaminant mixtures, has garnered much attention in both human health

58 and ecological risk assessments (Carpenter et al. 2002; Yang et al. 2007; Wang et al. 2008) with
59 the general recognition that the relationship among these mixture components and their
60 biological effects is both intricate and complex (Sexton et al. 2007). For heavy metal mixtures
61 this complexity is driven in part by the fact that many of these metals interact with a wide but
62 common set of cellular targets, but may differ in affinity for these targets by many orders of
63 magnitude (Viarengo 1989a).

64 We hypothesized that the relationship among heavy metals and their physiological effects
65 might be detected and modelled using a combination of linear and artificial neural network
66 (ANN) approaches. ANNs have been used to develop predictive models of other complex
67 systems such climate change (Cannon et al. 2002, among others) and disease status in humans
68 based upon gene expression profiles (Khan et al. 2001; Linder et al. 2004; Dankbar et al. 2007,
69 among others).

70 To test this hypothesis, we characterized the physiological effects of environmentally-
71 relevant low-dose mixtures of Cu, Cd, and Zn (Sanger et al. 1999), either alone or in
72 combination for periods from 1 – 27 days, in the Eastern oyster, *Crassostrea virginica*. This
73 ecologically and economically important bivalve mollusc lives in close association with
74 estuarine sediments where its sessile nature and filter-feeding habit maximize the accumulation
75 of contaminants in their tissues in concentrations high above those found in the surrounding
76 seawater (Jenny et al. 2002).

77 In oysters, as in other organisms, Cu, Cd and Zn exist as divalent cations which are free or
78 complexed to different classes of biological ligands. Cd is a trace metal with no known
79 biological function, while Cu and Zn are essential elements and, as such, are required to maintain
80 cellular homeostasis. In oysters, the gill and the hepatopancreas (digestive gland) are the
81 primary tissues involved in the accumulation and detoxification of heavy metals, such as Cu, Zn
82 and Cd (Marigómez et al. 2002; Sokolova et al. 2005). Heavy metals enhance the intracellular
83 formation of toxic reactive oxygen species (ROS) (Stohs et al. 1995b; Ringwood et al. 1998;
84 Geret et al. 2002b; Dailianis et al. 2005). Thus, metal-binding proteins and antioxidant enzymes,
85 such as glutathione (GSH) and metallothioneins (MTs) are important detoxification elements that
86 are induced to maintain the balance between pro- and antioxidative systems in cells (Dovzhenko
87 et al. 2005). Indeed, studies have shown that surplus ROS can alter the structure of cell
88 membranes by stimulating the peroxidation of membrane lipids. Thus, for the present study,

89 oysters were exposed to Cd, Zn, or Cu, either alone or in combination, for periods from 1 – 27
90 days and indicators of antioxidant defense (GSH), oxidative damage (lipid peroxidation; LPx),
91 immunocompetence (total hemocyte counts, numbers of invasive bacteria), as well as blood gas
92 and acid-base balance (hemolymph PO₂, pH, total CO₂) were measured for each animal. The
93 experimental design optimized input data for ANN analysis, which requires little or no
94 understanding of the mechanistic associations of the measured variables, but does require
95 considerable volumes of data. This design contrasts with traditional statistical approaches which
96 require extensive knowledge of the system, but comparatively little data. Perhaps more
97 succinctly traditional linear analysis fits data to models, but ANN's extracts models from data.
98 ANN's do not require independence among the input variables (independent variables in linear
99 regression). Furthermore, in the application of machine learning approaches, the preference is for
100 limited or no replication of the experimental conditions, so the ANNs learn rather than
101 memorize. For these and other reasons they have been used extensively in medical, engineering,
102 physics and atmospheric sciences (Almeida, 2002, Cannon et al. 2002 Khan et al. 2001; Linder
103 et al. 2004; Dankbar et al. 2007, Chapman *et al.* 2009) . Detailed explanations of the approach
104 can be found in Bishop (1996a,b Bishop 2006). Our approach was a compromise between the
105 requirements of linear statistics and of machine learning provided by ANNs. First, correlations
106 among the experimental variables were examined by linear statistical tools to provide statistical
107 power. Subsequently, ANN analysis was employed to explore the higher dimensional
108 interactions among metal mixtures on the oyster's physiological response.

109

110 **2. Materials and Methods**

111

112 *2.1. Animal collection and maintenance*

113

114 Adult Eastern oysters, *Crassostrea virginica* (Gmelin), from Taylor Shellfish Farms
115 (Shelton, WA) were held for 30 days in well-aerated recirculating natural seawater systems at 25
116 ppt salinity and 20 – 22 ° C on a 12 h light cycle. During this period oysters were fed a mixed
117 algal suspension (Shellfish Diet 1800[®], Reed Mariculture) every second day.

118

119 *2.2. Basic experimental protocol*

120

121 One day prior to the start of the experiment, 4 oysters were placed in each of 54 five L
122 beakers. Beakers contained four L of well-aerated filtered (0.45 μm) seawater maintained at 25
123 ppt salinity and 18 ± 1 °C. At the start of the 27 day experiment (Day 0), beakers were dosed
124 with single or multiple metals at environmentally relevant doses (Table 1): Cd (0.001 – 0.400
125 μM), Zn (0.001 – 3.059 μM) or Cu (0.002 – 0.787 μM). Thereafter, the seawater in each beaker
126 was routinely exchanged every second day, at which time metals were replenished in each
127 beaker to their predetermined concentrations, and algal suspension added to facilitate metal
128 uptake by the oysters. Food was withheld from oysters at least 24 h before they were sampled.

129 Sampling of oysters began on day 1 of the 27 day metal study, with 1 oyster sampled per day
130 from each of 8 beakers. Sampling began with beaker number one and continued to beaker 54,
131 then back to beaker one, continuing for 27 days until all 216 samples had been exhausted. The
132 study design was not consistent with a typical dose-response model based on linear statistics;
133 instead this design generated 216 individual treatments that ultimately could be analyzed by
134 ANNs. A total of 8 animals were found dead or moribund at the time of sampling; these oysters
135 were not associated with any particular dosing regimen and were excluded from the study.

136 Each sampled oyster was blotted dry with a paper towel and weight, length, and width were
137 recorded. Hemolymph (2 separate samples) was sampled anaerobically from the adductor
138 muscle of each oyster using a 1 mL glass syringe fitted with a 23-ga needle. The dead space in
139 the needle and syringe was filled with nitrogen-saturated distilled water to reduce contamination
140 of the sample by atmospheric oxygen; the syringe was placed on ice prior to sampling. To gain
141 access to the adductor muscle, the shell of the oyster was quickly notched along the posterior
142 margin using pliers, exposing the muscle. Immediately following hemolymph withdrawal,
143 oysters were placed on ice for dissection and tissue processing. Specific procedures are
144 described below.

145

146 2.3. *Quantification of total hemocyte count (THC) and culturable bacteria in hemolymph*

147

148 Approximately 0.5 mL of hemolymph was withdrawn from the adductor muscle of each
149 oyster. An aliquot of this sample was fixed with neutral buffered formaldehyde and hemocytes
150 counted with a hemocytometer (Macey et al. 2008). For total counts of culturable bacteria, a

151 second aliquot of the original hemolymph sample was overlaid in marine agar on TSA
152 supplemented with 2.0% NaCl; for total culturable *Vibrio*, a second 100 μ L aliquot of
153 hemolymph was overlaid in marine again and cultured on TCBS agar supplemented with 1.5%
154 NaCl (Macey et al. 2008). Data were expressed as total bacteria and *Vibrio* spp. mL^{-1} of
155 hemolymph according to growth on TSA and TCBS plates, respectively.

156

157 2.4. *Hemolymph variables*

158

159 A second hemolymph sample was withdrawn from the adductor muscle of each oyster to
160 assess hemolymph gas and acid-base chemistry. All instruments were thermostatted to 18 ± 0.1
161 $^{\circ}\text{C}$. The partial pressure of oxygen (PO_2) in the hemolymph was determined with a Radiometer
162 PHM pH/blood gas monitor and PO_2 electrode. Hemolymph pH was determined with a
163 Radiometer (BMS2 Mk2 Blood Micro System) capillary pH electrode and PHM pH/blood gas
164 monitor that had been calibrated at experimental temperatures with precision Radiometer buffers.
165 Total carbon dioxide, i.e., all forms of CO_2 including molecular CO_2 , HCO_3^- , $\text{CO}_3^{=}$, and
166 carbamino CO_2 , in the hemolymph was determined with a Capni-Con 5 total CO_2 analyzer
167 (Cameron Instrument Company).

168

169 2.5. *Oyster dissection and tissue processing.*

170

171 The right valve of each oyster was removed by breaking the hinge of the shell and
172 removing the gills and the hepatopancreas to separate weigh boats. Tissues were minced and
173 approximately 0.02 g (minimum) and 0.05 g (maximum) samples of the minced tissues were
174 transferred to separate cryotubes, flash frozen in liquid nitrogen and stored at -80°C until they
175 were used for the GSH, LPx and metal content assays (see below).

176

177 2.6. *Lipid peroxidation (LPx) and glutathione (GSH) assays.*

178

179 Lipid peroxidation (LPx) in the gill and hepatopancreas of *C. virginica* was measured
180 using a colorimetric assay that quantifies lipid degradation products based on the formation of
181 total thiobarbituric acid reactive substances (TBARS) with malondialdehyde (TBARS) as the

182 standard (Ringwood et al. 1999b). GSH concentrations of individual oyster tissues were
183 determined using the glutathione reductase recycling assay described by Ringwood et al.
184 (1999b).

185

186 2.7. *Analysis of metal content*

187

188 Tissues were digested in concentrated nitric acid at 160 °C at 210 psi and 225 watt for 6
189 min. Cooled samples were spiked with yttrium standard (10 ppm final concentration) and
190 analyzed for Cu, Cd and Zn content by Inductively Coupled Plasma-Atomic Emission
191 Spectroscopy. The National Bureau of Standards (NBS) Mussel Reference Material #1974b and
192 Pygmy Sperm Whale Reference Material # QC03-LH3 were analysed with the samples to verify
193 the metal analysis; the percent recoveries over all batches were 101.67 ± 11.74 , 101.87 ± 11.14 ,
194 and $99.00 \pm 10.99\%$ (mean \pm S.D.) for Cu, Zn and Cd, respectively, for the Whale Reference
195 Material and 106.78 ± 5.52 , 95.74 ± 4.70 , and $106.97 \pm 9.21\%$, respectively, for the Mussel
196 Reference Material. .

197

198 2.8. *Statistical analysis.*

199 . To determine the effect of metal exposure on the tissue accumulation of each metal and to
200 assess potential relationships between tissue metal content and physiological responses, data
201 were analyzed initially by linear statistics using SigmaStat 3.1 and SYSTAT 11 software.
202 Correlations between tissue content of each metal and physiological measures were investigated
203 using Pearson's Product Moment Correlation procedure. All tests for normality (Kolmogorov-
204 Smirnov test) or equal variances failed, therefore, correlation analyses were performed on rank
205 transformed data. One-way ANOVA was used to test for differences in concentrations of each
206 metal between the gills and the hepatopancreas of oysters exposed to metals and was also used to
207 test for differences between basal concentrations of each metal in each tissue of oysters not
208 exposed to metals. All tests for normality or equal variances failed, therefore, a Kruskal-Wallis
209 ANOVA on Ranks test was used to test for significant differences. Interactions between metal
210 content of each tissue and physiological responses were assessed by analysis of variance
211 (ANOVA) using General Linear Models (GLM) in SYSTAT 11. Since all test for normality and
212 equal variance failed, GLM on quantile-normalized data were used to test for significant

213 interactions. Each GLM consisted of 3 independent variables [tissue (gill or hepatopancreas) Cu,
214 Zn and Cd] and one dependent variable [tissue (gill or hepatopancreas) TBARS]. Significance
215 was assigned at $p \leq 0.05$ for all analyses. Subsequently, ANNs were used to model potential
216 interactions of tissue metal contents and hemolymph measures in predicting tissue oxidative
217 damage (LPx) or antioxidant status (GSH). Each of the ANNs consisted of 6 input variables
218 [hemolymph pH, total CO₂, PO₂, and tissue (gill or hepatopancreas) Cu, Zn and Cd] with one
219 output variable. For each output variable (gill LPx, gill GSH, hepatopancreas LPx and
220 hepatopancreas GSH), separate ANNs (n = 30) were developed using WebNeuralNet 1.0
221 (Almeida 2002). All variables were scaled to their non-parametric cumulative distributions by
222 replacing the raw values with their rank/n (n = total data points) to overcome scale differences.
223 The transformed data were then divided into two sets by random allocation; one comprising 90%
224 of the records to train the ANN, while the remaining data were used as a cross validation (CV)
225 set. A new subset of data was randomly selected before training each ANN to avoid bias in the
226 selection of the CV set. Each ANN was first trained using both the input and output data of the
227 training set, which consisted of 187 data points from each of the input and output variables. To
228 prevent over training the ANNs, an early stopping procedure (Almeida 2002) was employed.
229 After each ANN was trained, the withheld data points from the CV set were analyzed to evaluate
230 the predictive capabilities of the ANN. In essence, this was achieved by calculating the R-
231 squared (R²) values for the outputs of each ANN and the observed values of the accompanying
232 CV sets, and comparing the CV set predictions with those generated by the appropriate ANN.
233 Next, the impact of each input variable (hemolymph pH, total CO₂, PO₂, tissue Cu, Cd, Zn) was
234 examined by computing the sensitivities of the outputs to changes in the inputs (Heshem, 1992)
235 for all ANNs in which the model and CV set R² value were greater than the median value for all
236 30 ANNs. The interactions of the inputs on the outputs were examined using a derivative of the
237 approach of Cannon and McKendry (2002), where the two variables with the highest sensitivities
238 were allowed to vary in 5% increments over the scaled range and all other input variables were
239 held to their mean (50%) values. These ‘artificial’ data were then fed to the ANN models with
240 the largest R² values to predict the output value and the results plotted on three-dimensional
241 surfaces.

242

243 **3. Results**

244

245 3.1. *Metal accumulation in the tissues of C. virginica.*

246

247 Overall, measured concentrations of Cu, Cd and Zn ($\mu\text{g g}^{-1}$ wet weight tissue) were
248 higher in the hepatopancreas than in the gills of oysters exposed to metals (one-way ANOVA; P
249 < 0.001 , < 0.001 , $= 0.003$ and for Cu, Cd and Zn, respectively). Furthermore, basal
250 concentrations of Cu and Zn were noticeably higher and more variable in the gills and the
251 hepatopancreas when compared to basal Cd concentrations ($P < 0.001$). Tissue levels of the
252 essential metals Cu and Zn were independent of the ambient water concentrations of the metals
253 over the entire range of exposures (Fig. 1A, B). In contrast, cadmium, a non-essential metal, was
254 the only metal that accumulated linearly with time in the gill ($r = 0.828$; $P < 0.001$) and the
255 hepatopancreas ($r = 0.793$; $P < 0.001$) over the full range of Cd exposure concentrations (Fig.
256 1C). Cu contents were directly related to those of Zn in the gill ($n = 208$, $r = 0.0713$, $P < 0.001$)
257 and in the hepatopancreas ($n = 208$, $r = 0.649$, $P < 0.001$). To a lesser degree, Cu content
258 positively correlated with Cd content in the gill ($r = 0.216$, $P = 0.0018$), but not in the
259 hepatopancreas. No other significant correlations were observed between measured metals in
260 either tissue.

261

262 3.2. *Correlation of measured tissue metals with physiological traits of C. virginica.*

263

264 Since each of the 216 test animals represented a unique set of metal exposure parameters
265 (combination of metals, dose levels and duration), the resulting values could not be represented
266 by standard descriptive statistics. Physiological data obtained from the 216 test animals (Figure
267 2) generally fell within ranges reported for *C. virginica* in control or low level metal exposures
268 (Viarengo et al. 1990; Roméo et al. 1997; Ringwood et al. 1998; Ringwood et al. 1999a).
269 Correlations between metal exposures and physiological measures were investigated using
270 Pearson's Product Moment Correlation procedure. Exposure to Zn was negatively correlated
271 with TBARS, indicators of oxidative membrane damage in the hepatopancreas, ($r = -0.150$, $P =$
272 0.0304), but not in the gill. No other significant relationships were noted between metal
273 exposures and physiological measurements in oysters (data not shown). In contrast, tissue
274 concentrations of individual metals were associated with several physiological measurements

275 (Fig. 3A, B), most notably TBARS. In the gill, Cu ($r = 0.527$, $P < 0.001$), Cd ($r = 0.204$, $P =$
276 0.0032) and Zn ($r = 0.256$, $P < 0.001$) correlated positively with TBARS, as did Cu ($r = 0.618$, P
277 < 0.001) and Zn ($r = 0.247$, $P < 0.001$) in the hepatopancreas. By comparison, metal associations
278 with GSH were mixed. In the gill only Cu ($r = 0.203$, $P = 0.0033$) but not Zn or Cd positively
279 correlated with antioxidant GSH, while both Cd ($r = -0.149$, $P < 0.001$) and Zn ($r = -0.95$, $P =$
280 0.0049) in the hepatopancreas were negatively associated with GSH in that tissue.

281 Several other significant correlations were noted (Fig. 3A, B). Gill Cd was associated
282 with increased hemolymph pH ($r = 0.159$, $p = 0.0221$) while hepatopancreas Cu correlated with
283 increased hemolymph pH (and $r = 0.284$, $P < 0.001$, respectively) and decreased total CO₂ ($r =$
284 -0.137 , $P = 0.0477$). Of the three metals, only Cu was associated with markers of immune
285 function. Gill Cu was positively correlated with total culturable bacteria in the hemolymph ($r =$
286 0.138 , $P = 0.0461$), while hepatopancreas Cu was negatively associated with THC ($r = -0.180$, P
287 $= 0.0092$).

288 In the hepatopancreas there was a significant interaction between measured Cu and Zn
289 when predicting oxidative damage, measured as TBARS (Table 2, GLM, $P = 0.014$), but not in
290 the gill tissue. No additional significant interactions between the content of metals measured in
291 gill and hepatopancreas were evident when predicting other physiological measurements of
292 oysters, such as GSH, THC, hemolymph pH or total CO₂.

293

294 3.3. *Artificial neural network analysis (ANN).*

295

296 Because interactions among the metals were detected by linear analysis, ANNs were used
297 to explore these interactions in predicting LPx (measured as TBARS) in contrast to predicting
298 GSH in the hepatopancreas and gill. The three respiratory measurements hemolymph pH, total
299 CO₂ and PO₂ were included as input variables because the two acid-base components (pH, total
300 CO₂) responded to tissue contents of all three metals. ANN models could more reasonably
301 predict hepatopancreas than gill TBARS based on the metal content of the respective tissues.

302 The mean R² value for hepatopancreas TBARS over all the ANN models was 0.50 ± 0.11 (Mean
303 \pm SD, $n = 30$), with some of the values approaching 0.7 (Table 3). By comparison, the mean R²
304 value for gill TBARS over all models was 0.35 ± 0.11 (Table 4). Similarly, the cross-validation
305 R² values for models predicting TBARS were 0.53 ± 0.14 (Table 3) and 0.24 ± 0.16 (Table 4) for

306 the hepatopancreas and the gills, respectively, confirming the relative validity of the predictions
307 made by each model. Furthermore, hepatopancreas TBARS appeared to be more consistently
308 predictable than gill TBARS, as the variation in R^2 and cross-validation R^2 values with respect to
309 the mean in each model were smaller for the hepatopancreas than for the gills (Tables 3, 4).

310 In contrast, GSH in both the gills and the hepatopancreas was poorly predicted by the
311 input variables used for ANN modelling. The mean R^2 values for predicting GSH were only
312 0.07 ± 0.06 (Table 3) and 0.14 ± 0.11 (Table 4) for the gills and the hepatopancreas, respectively.
313 Likewise, the mean cross-validation R^2 values and their variances for models predicting GSH in
314 both tissue types were very low (Tables 3, 4).

315 A sensitivity analysis was conducted for the top performing ANNs to determine the
316 contribution of each of the 6 input variables [hemolymph pH, total CO_2 , PO_2 , and tissue (gill or
317 hepatopancreas) Cu, Cd or Zn] to the overall variance observed in each model predicting tissue
318 TBARS. As GSH was poorly predicted by all ANN models in the present study, a sensitivity
319 analysis was not conducted for these models. The best performing ANNs had model and cross-
320 validation R^2 values greater than the median value for all 30 ANNs. Models 6 and 7 were chosen
321 from the ANNs predicting hepatopancreas TBARS (Table 3), while Model 8 was chosen from
322 ANNs predicting gill TBARS (Table 4). Sensitivity analysis reveals that in the hepatopancreas,
323 the partial pressure of oxygen (PO_2) in the hemolymph is a dominant variable in both models
324 (Fig. 4). Model 6 has the larger mean R^2 value. Model 7 has the larger cross-validation R^2 value
325 and a smaller number of nodes (Table 4) and in most cases we would choose Model 7 over 6 for
326 these reasons. However, as Model 6 indicates that Cu is more important than Zn in predicting
327 TBARS (indicating LPx) and as this model confirms findings from the linear statistical analysis,
328 we would suggest that this is the preferred ANN model. Model 6 suggests that LPx in the
329 hepatopancreas is more sensitive to changes in tissue Cu and Cd, and to hemolymph PO_2 , than to
330 any of the other measured variables (Fig. 4).

331 Sensitivity analysis indicated that each of the input variables contributed to the overall
332 variance observed in Model 8 in predicting gill TBARS (Fig. 5). In the gill, as in the
333 hepatopancreas, it is clear that the degree of oxidative membrane damage is more sensitive to
334 changes in tissue Cu than to other input variables, but hemolymph pH, total CO_2 and PO_2 also
335 make strong contributions to predicting TBARS. Moreover, summed Cu, Zn and Cd
336 concentrations in both tissues appear to make significant contributions towards the overall

337 variance observed in each model, emphasizing the cumulative detrimental effects of these metals
338 on membrane integrity.

339 The interactions of the more sensitive input variables (tissue Cu, hemolymph pH and
340 hemolymph PO₂) in predicting TBARS in the gills and the hepatopancreas were graphically
341 illustrated (Fig. 6A, B) using a modified form of the sensitivity analysis described by Cannon
342 and McKendry (2002). Oxidative damage in the gill (TBARS) increased as hemolymph pH and
343 tissue Cu concentrations increased and the effects are non-linear, but not strongly so (Fig. 6A).
344 Similarly, hepatopancreas TBARS increased with increasing PO₂ in the hemolymph and with
345 hepatopancreas Cu (Fig. 6B). These graphical surfaces clearly suggest complex, non-linear
346 interactions between tissue Cu content and hemolymph pH or PO₂ in predicting tissue TBARS.
347 Furthermore, the overall TBARS response is consistent with an increasingly oxidative
348 environment.

349

350 **4. Discussion**

351

352 ANN models generated in the present study demonstrated that the responses of key
353 toxicological indicators can be modelled and predicted from an appropriate set of input variables.
354 While linear analyses provided correlative values of some individual metals to changes in
355 hemolymph gasses and pH, ANN analysis suggested that the level of damage to cellular
356 membranes was sensitive to tissue content of all three metals and strongly depended on other
357 physiological measures, such as changes in hemolymph pH and PO₂ (Fig. 6). To our knowledge,
358 this is the first study to show important metal-metal interactions as well as interactions of metal
359 content with hemolymph gas and acid-base chemistry in predicting membrane damage in
360 molluscs. It is particularly noteworthy that where low tissue Cu is accompanied by low pH or
361 low PO₂ both hepatopancreas and gill manifest the lowest predicted level of TBARS, while in
362 those tissues with high Cu content along with high pH or high PO₂, the reverse is observed (Fig.
363 6). This is in keeping with our understanding of the response of TBARS to redox conditions,
364 and the overall topography of the predicted response clearly suggests a non-linear interaction
365 between metal content, hemolymph acid-base variables and TBARS. The contributions of
366 hemolymph variables to the predictive power of the ANN models as observed in the present
367 study could be explained by changes in ventilation rate of oysters as function of metal exposure

368 or tissue burden, as reported for tropical oysters *Crassostrea belcheri* exposed to Cu (Elfwing et
369 al. 2002). Alternatively, tissue metal burdens may be limited by ventilatory activity in bivalves
370 as reported for Cd uptake in the Asiatic clam, *Corbicula fluminea* (Massabuau et al. 2003).
371 Certainly, the resulting changes in gas exchange and acid-base physiology of oysters could
372 influence a variety of biochemical processes, including the deposition of shell that is essential to
373 oyster growth (Booth et al. 1984; Burnett 1988).

374 While linear regression techniques can generate response-surface plots, they cannot
375 interrogate non-linear dynamics similar to those in Fig 6 without human intervention specifying
376 the structure of the relationships. The advantage of the ANN's is that the mathematical
377 architecture is infinitely flexible and does not require human intervention (eg. bias). The various
378 models produced by the analysis are not viewed as solutions, but rather as hypotheses of
379 relationships amenable to further empirical tests.

380 In the present study, Cu, Zn and Cd tissue contents correlated with significant changes in
381 LPx, as measured by elevated tissue levels of total TBARS. The influence of transition metals
382 such as Cu on oxidative processes, resulting in the production of oxyradicals, has been described,
383 and it is suggested that cupric ions are involved in both the initiation and propagation steps of
384 LPx (reviewed by Viarengo 1989a). In fact, increases in LPx following exposure to Cu have
385 been documented in the hard clam *Ruditapes decussatus* (Roméo et al. 1997), the Eastern oyster
386 *Crassostrea virginica* (Ringwood et al. 1998), and the mussels *Mytilus galloprovincialis*
387 (Viarengo et al. 1990) and *Mytilus edulis* (Geret et al. 2002a). While excess Cu can mediate free
388 radical production directly via redox cycling, oxyradicals may also be formed indirectly via
389 cupric ions binding to and adversely affecting metal-requiring antioxidants, such as GSH and
390 MT (Ringwood et al. 1999a; Valko et al. 2005). In fact, it has been strongly suggested that there
391 are multiple processes that bind copper and reduce its cellular toxicity (Valko et al. 2005).
392 Conversely, non-redox metals, such as Cd, are unable to generate free radicals directly and
393 indirectly cause free radical-induced damage to important cellular macromolecules, particularly
394 various complexes of the electron transport chain in mitochondria, and inhibit important cellular
395 antioxidant enzymes and proteins, which may, in turn, stimulate LPx through oxidation of
396 polyunsaturated fatty acids (Stohs et al. 1995a; Stohs et al. 2000; Dorta et al. 2003; Wang et al.
397 2004). The inverse association of Zn and Cd with GSH in the hepatopancreas observed in our
398 study supports the idea that GSH provides early protection against oxidative stress from

399 exposure to these metals, by binding of these metals to GSH or inhibition of GSH synthesis by
400 these metals, until MTs can be induced (Quig 1998; Ringwood et al. 1998). That this effect was
401 not noted for Cu in this study supports the notion that Cu ions, which can undergo redox cycling,
402 are involved in both the initiation and propagation steps of LPx via the direct formation of
403 reactive oxygen species, whereas Cd and Zn ions, which do not undergo redox cycling, stimulate
404 LPx indirectly by binding to and inhibiting cellular antioxidants, such as GSH (Viarengo 1989a).
405 This does not however exclude the possibility of the formation of Cu-GSH complexes,
406 particularly since –SH groups of most metabolites and enzymes, including GSH, have a higher
407 affinity for Cu than Cd or Zn (Viarengo 1989b). In fact, the discovery that the upper limit of
408 “free” pools of Cu are far less than a single ion per cell strongly suggests that there is significant
409 overcapacity for chelation of Cu in the cell and that multiple cellular antioxidants exist that bind
410 Cu (Valko et al. 2005). However, Ringwood et al. (Ringwood et al. 1998) suggested that
411 conditions that cause depletion of important cellular antioxidants, such as GSH and MT, may
412 enhance pollutant toxicity, suggesting that the impacts of exposure to metal mixtures are
413 complex and potentially compounding. Indeed, the significant correlation between tissue
414 contents of Cd and LPx as well as the general linear model identification of Zn-Cu interactions in
415 predicting LPx of oysters in the present study supports this notion.

416 Cd suppresses the activity of many antioxidant enzymes and can displace Cu and Fe from
417 cytoplasmic and membrane proteins which may then participate in ROS-producing Fenton
418 reactions (Flipič et al. 2006). More specifically, Engel (1999) demonstrated that Cu can displace
419 Cd from MT when oysters are exposed to these trace metals in combination, but that Cd is not
420 lost from the tissues of the oyster. Furthermore, it is postulated that MT gene expression in
421 oysters is regulated via a Zn-sensitive inhibitor, as is the case for regulation of MT gene
422 expression in mice (Roesijadi 1996). Although MT induction via the displacement of Zn has yet
423 to be empirically demonstrated in oysters, it is possible that this sort of metal-metal exchange
424 reaction is responsible for the Zn-Cu interactions observed in oysters in the present study when
425 predicting tissue LPx.

426 The approach of combining general linear models and ANN analysis has revealed
427 important metal-metal interactions as well as interactions of metal content with hemolymph gas
428 and acid-base chemistry (hemolymph PO₂ as well as pH and total CO₂) in predicting peroxidation
429 of membrane lipids that were not evident from linear analyses. These results support a growing

430 body of evidence implicating the role of heavy metals in the peroxidation of membrane lipids
431 and the disruption of important cellular antioxidants that play key roles in protecting cells against
432 oxidative damage. This study also highlights the usefulness of machine learning approaches,
433 such as ANNs, for improving our ability to recognize and understand the effects of sub-acute
434 exposure to environmentally relevant concentrations of mixed contaminants.

435

436 **5. Acknowledgements**

437

438 This study was supported by NOAA's Center of Excellence in Oceans and Human Health
439 at HML and the National Science Foundation. Any opinion, finding, conclusions or
440 recommendations expressed in this material are those of the authors and do not necessarily
441 reflect the views of the NSF. GML Contribution No. 348; MRD SCDNR Contribution ####.

442

443 **Tables**

444 **Table 1.** Concentrations (μM) of CuCl_2 , ZnCl_2 and CdCl_2 added to each beaker during the 27
 445 day oyster metal challenge experiment.

446	Beaker #	Zinc	Copper	Cadmium
447	1	0.049	0.000	0.214
448	2	0.196	0.315	0.000
449	3	0.306	0.002	0.037
450	4	1.101	0.066	0.044
451	5	3.059	0.044	0.010
452	6	0.000	0.000	0.000
453	7	2.447	0.050	0.000
454	8	0.000	0.197	0.013
455	9	0.092	0.000	0.062
456	10	0.000	0.000	0.025
457	11	0.306	0.079	0.000
458	12	1.835	0.598	0.267
459	13	1.590	0.787	0.002
460	14	0.000	0.039	0.004
461	15	1.223	0.017	0.231
462	16	2.080	0.000	0.004
463	17	0.000	0.010	0.006
464	18	0.000	0.000	0.000
465	19	0.765	0.000	0.111
466	20	0.000	0.220	0.400
467	21	0.040	0.000	0.044
468	22	0.000	0.000	0.000
469	23	0.000	0.000	0.302
470	24	0.979	0.409	0.000
471	25	0.031	0.008	0.004
472	26	0.171	0.504	0.178
473	27	0.428	0.000	0.000
474	28	0.000	0.252	0.445
475	29	0.015	0.004	0.125
476	30	0.012	0.000	0.000
477	31	0.000	0.000	0.160
478	32	0.110	0.028	0.016
479	33	1.468	0.110	0.001
480	34	2.325	0.007	0.000
481	35	0.006	0.472	0.320
482	36	2.753	0.000	0.000
483	37	0.000	0.003	0.000
484	38	0.000	0.013	0.338
485	39	0.000	0.001	0.000
486	40	2.202	0.000	0.028
487	41	0.000	0.157	0.007

488	42	0.000	0.024	0.356
489	43	0.003	0.000	0.000
490	44	0.028	0.283	0.000
491	45	0.067	0.567	0.007
492	46	0.000	0.708	0.000
493	47	0.153	0.006	0.000
494	48	0.612	0.000	0.089
495	49	0.000	0.079	0.000
496	50	1.957	0.629	0.285
497	51	0.049	0.013	0.142
498	52	0.257	0.535	0.002
499	53	0.856	0.378	0.000
500	54	0.024	0.000	0.022
501				

502 **Table 2.** Assessment of interactions between metal contents of hepatopancreas when predicting
 503 oxidation damage, measured as TBARS (General Linear Models). * significant interactions
 504 (P<0.05).

505	506	Coefficient	STD Error	STD	Tolerance	t	P(2 Tail)
507				Coefficient			
508	Constant	2.894	10.174	0.000	.0284	0.777	
509	Cu	1.309	0.416	1.309	0.045	3.149	0.003*
510	Zn	0.777	0.399	0.777	0.049	1.949	0.056
511	Cd	-0.043	0.276	-0.043	0.102	-0.156	0.877
512	Cu*Zn	-0.026	0.010	-1.668	0.018	-2.525	0.014*
513	Cu*Cd	-0.004	0.011	-0.207	0.024	-0.360	0.720
514	Zn*Cd	-0.015	0.011	-0.809	0.022	-1.346	0.183
515	Cu*Zn*Cd	0.00	0.000	1.251	0.011	1.515	0.135
516							

517 **Table 3.** ANN (n = 30) analysis of TBARS and GSH levels in the hepatopancreas of oysters
 518 exposed to Cu, Zn and/or Cd.

519	Lipid Peroxidation (TBARS)				Glutathione (GSH)		
520	Model	# Nodes	Model R2	CV R2	#Nodes	Model R2	CV R2
521	1	9	0.4289	0.2652	9	0.1349	0.0866
522	2	9	0.3715	0.7326	7	0.1441	0.1110
523	3	5	0.6957	0.3642	5	0.3667	0.1649
524	4	7	0.5006	0.4938	5	0.0864	0.0328
525	5	7	0.3917	0.6919	5	0.0720	0.2296
526	6	7	0.6465	0.4681	7	0.1176	0.1654
527	7	5	0.6072	0.7002	7	0.3028	0.0688
528	8	5	0.3979	0.6905	9	0.1172	0.3552
529	9	7	0.5649	0.7380	6	0.3948	0.0058
530	10	5	0.6035	0.6459	7	0.0586	0.1656
531	11	6	0.6075	0.5286	5	0.1056	0.2849
532	12	5	0.6124	0.6212	11	0.1279	0.3194
533	13	7	0.4208	0.8799	7	0.1111	0.0151
534	14	5	0.3779	0.5179	5	0.0775	0.0807
535	15	5	0.4201	0.6586	7	0.1033	0.2656
536	16	5	0.4052	0.5568	5	0.3134	0.3727
537	17	5	0.6587	0.3128	5	0.2803	0.1421
538	18	5	0.6269	0.4792	5	0.0992	0.1796
539	19	5	0.2801	0.5103	8	0.1201	0.1013
540	20	6	0.4136	0.5071	5	0.0255	0.2573
541	21	5	0.6408	0.3670	9	0.1422	0.0052
542	22	5	0.3890	0.5743	5	0.3510	0.4110
543	23	5	0.6245	0.4559	6	0.1006	0.0303
544	24	5	0.5942	0.4939	7	0.0676	0.0754
545	25	5	0.4384	0.4662	5	0.1239	0.0052
546	26	5	0.4184	0.4533	6	0.3116	0.0455
547	27	7	0.5060	0.5056	5	0.0111	0.0003
548	28	5	0.4105	0.6626	5	0.0197	0.0169
549	29	5	0.3373	0.3752	6	0.1104	0.0000
550	30	7	0.6149	0.2975	5	0.0427	0.0432
551	Mean	5.8000	0.5002	0.5338	6.3000	0.1480	0.1346
552	SD	1.2149	0.1178	0.1464	1.6006	0.1100	0.1247

553 **Table 4.** ANN (n = 30) analysis of TBARS and GSH levels in the gills of oysters exposed to
 554 Cu, Zn and/or Cd.

555	Lipid Peroxidation (TBARS)				Glutathione (GSH)		
556	Model	#Nodes	Model R2	CV R2	#Nodes	Model R2	CV R2
557	1	5	0.2538	0.0007	9	0.0797	0.0154
558	2	7	0.2423	0.1488	7	0.0179	0.0647
559	3	7	0.2578	0.4011	9	0.0635	0.0173
560	4	6	0.2405	0.1909	5	0.0029	0.0504
561	5	5	0.1802	0.3001	7	0.0314	0.0003
562	6	7	0.2687	0.4040	7	0.0726	0.0044
563	7	8	0.3386	0.2644	8	0.0843	0.0459
564	8	8	0.4818	0.2464	5	0.0471	0.0413
565	9	7	0.1684	0.0625	10	0.0697	0.0393
566	10	11	0.4871	0.2322	9	0.2961	0.0250
567	11	5	0.4528	0.2011	7	0.0223	0.1310
568	12	6	0.2826	0.4182	7	0.0674	0.0007
569	13	6	0.4153	0.4901	6	0.0178	0.1964
570	14	5	0.5444	0.0489	5	0.0526	0.0022
571	15	7	0.4401	0.1768	5	0.0498	0.1191
572	16	8	0.3297	0.2637	11	0.0588	0.0771
573	17	5	0.4234	0.4465	6	0.0650	0.1535
574	18	7	0.5074	0.1323	6	0.0344	0.0139
575	19	9	0.3102	0.1496	7	0.1644	0.0249
576	20	5	0.3989	0.4732	5	0.0346	0.0899
577	21	8	0.2456	0.3080	7	0.0346	0.0029
578	22	5	0.3934	0.5798	5	0.0758	0.0025
579	23	5	0.5077	0.0112	7	0.0554	0.0097
580	24	5	0.1863	0.2495	5	0.0793	0.0159
581	25	5	0.3005	0.0058	8	0.0431	0.0394
582	26	7	0.2522	0.1038	10	0.0694	0.0328
583	27	9	0.2899	0.3309	11	0.0732	0.0266
584	28	5	0.2295	0.2209	9	0.1984	0.0519
585	29	5	0.4402	0.5114	7	0.1516	0.0122
586	30	5	0.5173	0.0320	8	0.0652	0.1652
587	Mean	6.4333	0.3462	0.2468	7.2667	0.0726	0.0491
588	SD	1.5906	0.1139	0.1641	1.8370	0.0597	0.0536
589							

590 **Figure Legends**

591 **Figure 1.** (A) The tissue concentrations of Cu measured in the gill and the hepatopancreas of
592 *Crassostrea virginica* held in Cu alone or in combination with other metals for 1 – 27 days.
593 Total waterborne exposure to Cu (x-axis) is expressed as water concentration of Cu (μM) *days
594 of exposure. Concentrations of Zn (B) and Cd (C) in the same tissues are displayed as a
595 function of total waterborne exposure to Zn and Cd, respectively.

596

597 **Figure 2.** Box-and-whiskers plots of data from all experimental animals (n = 208) for each
598 major physiological variable measured in this study. (A) TBARS and GSH values for the gill
599 and the hepatopancreas (Hepato), (B) total hemocyte count (THC), (C) hemolymph PO_2 and total
600 CO_2 , (D) hemolymph pH, and (E) colony-forming units (CFU) mL^{-1} hemolymph on TSA or
601 TCBS agar. Box boundaries indicate 25th and 75th percentile, the line within the box marks the
602 median value, and whiskers indicate the 10th and 90th percentiles. All values, including outliers
603 are depicted.

604

605 **Figure 3.** Correlation coefficients (r-values) for significant associations between physiological
606 measurements and measured metals in (A) the gill and (B) the hepatopancreas of *Crassostrea*
607 *virginica* following exposure to each metal alone and in combinations for a period of 1 – 27
608 days. Analysis was performed using the Pearson Product Moment Correlation procedure on rank
609 transformed data and significance was assigned at $P < 0.05$. Non-significant interactions are not
610 shown.

611

612 **Figure 4.** Sensitivities of TBARS in hepatopancreas to the input variables (metal contents,
613 hemolymph pH, PO₂ and total CO₂) for the best performing models 6 and 7 from the ANN
614 analysis.

615

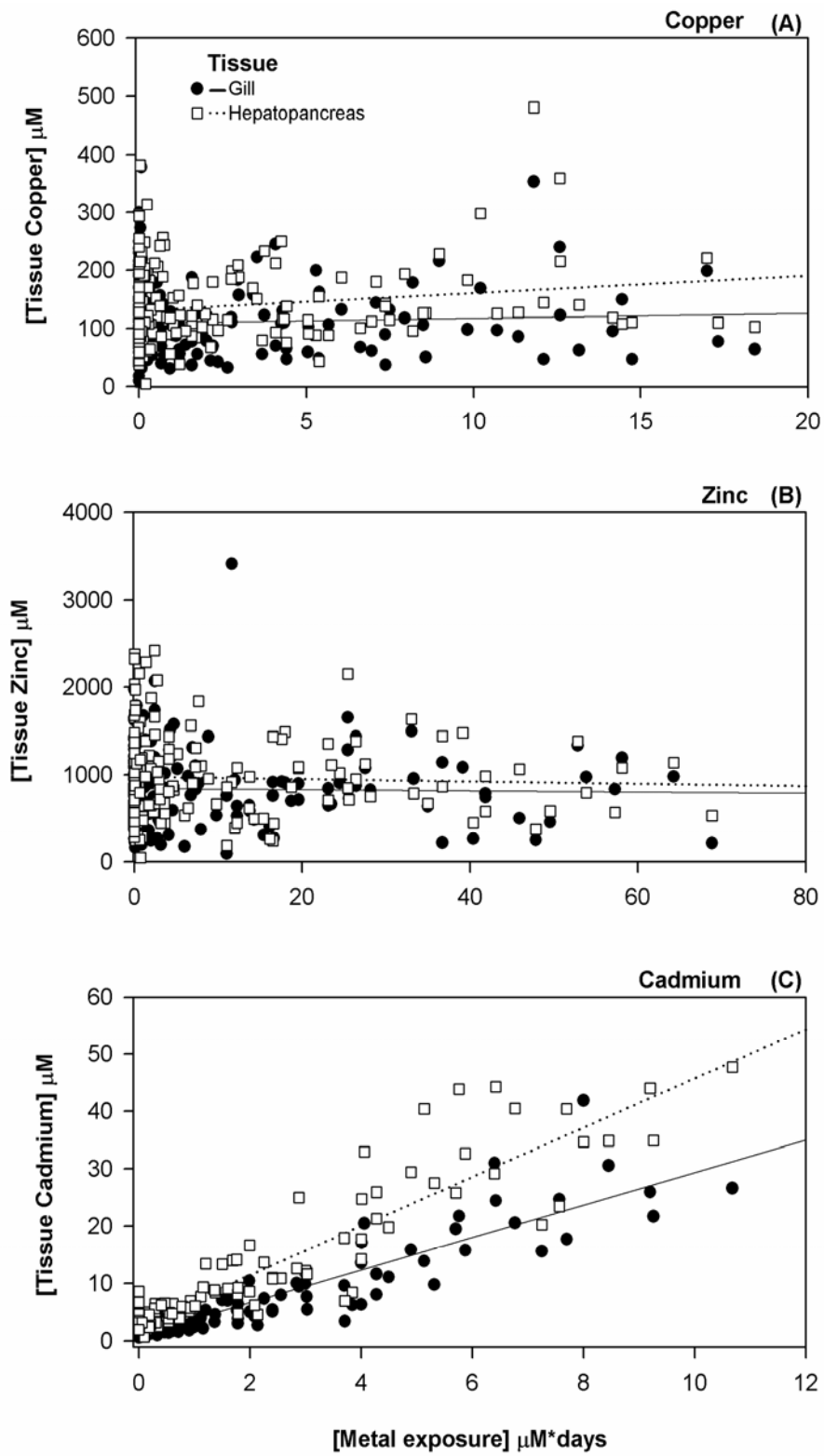
616 **Figure 5.** Sensitivities of TBARS in the gill to the input variables (metal contents, hemolymph
617 pH, PO₂ and total CO₂) for the best performing model 8 from the ANN analysis.

618 **Figure 6.** Theoretical projections of the response of TBARS to changes in the exposure levels of
619 the indicated variable on the x and y axes. All variables have been scaled to their non-parametric
620 values where 0 indicates the minimum and 1 indicates the maximum values observed in the data.
621 (see text).

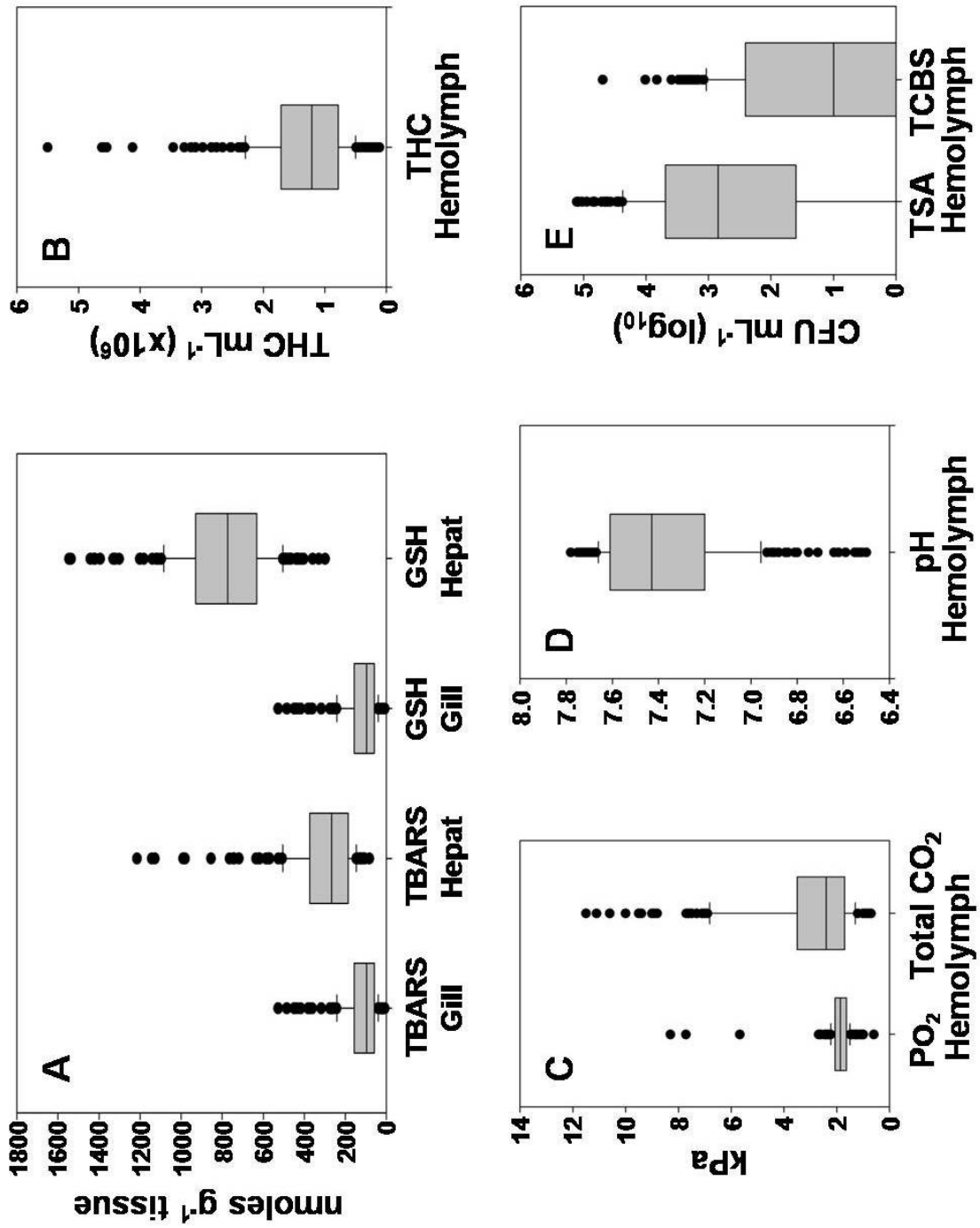
622

623

624 **Figure 1**
625
626

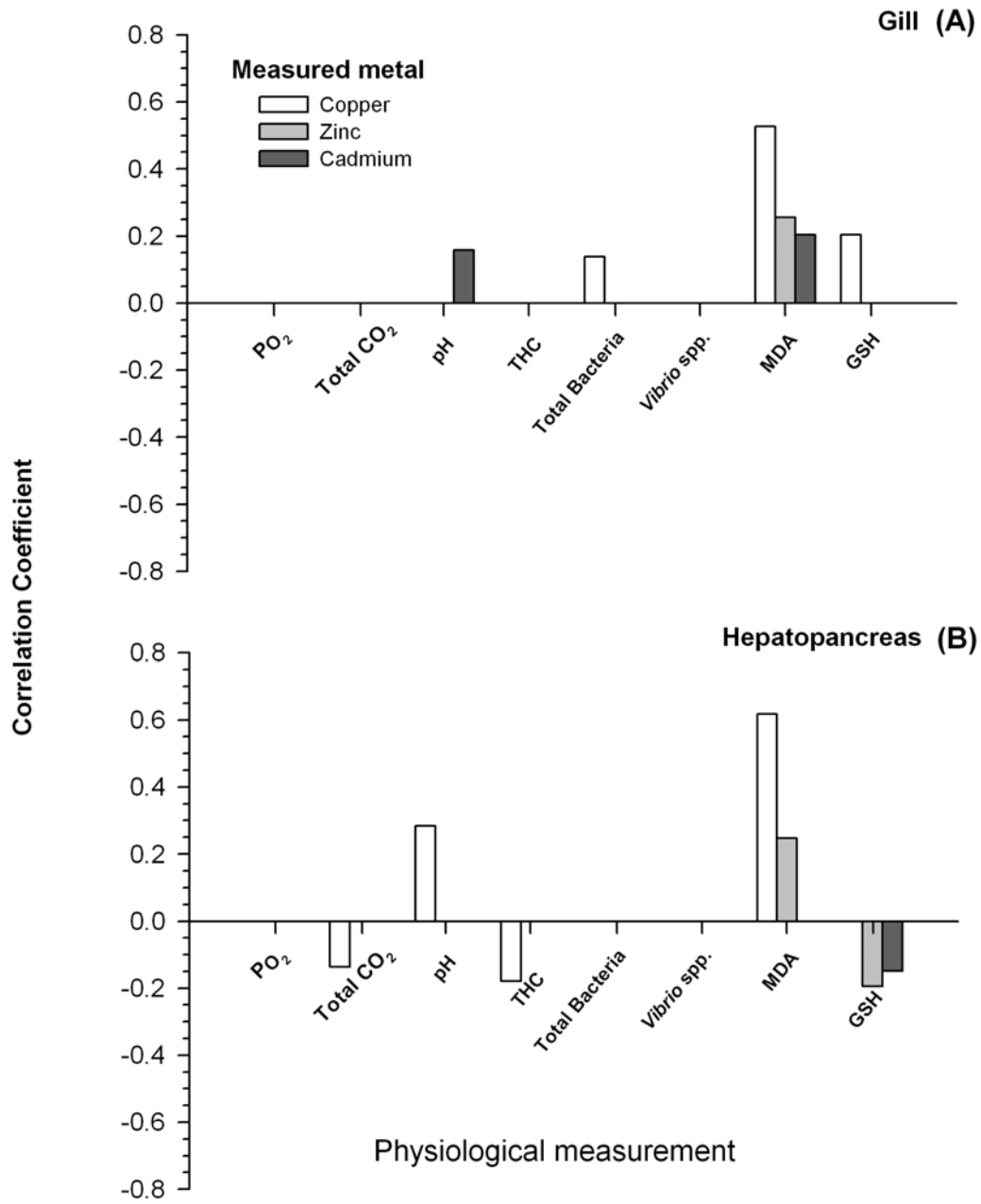


627 Figure 2
628



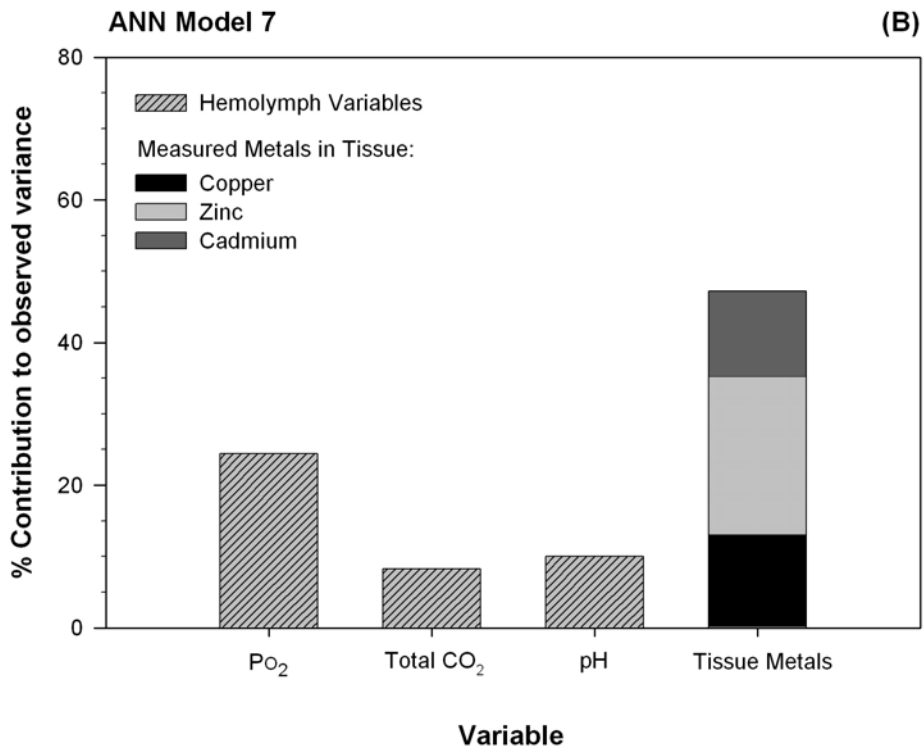
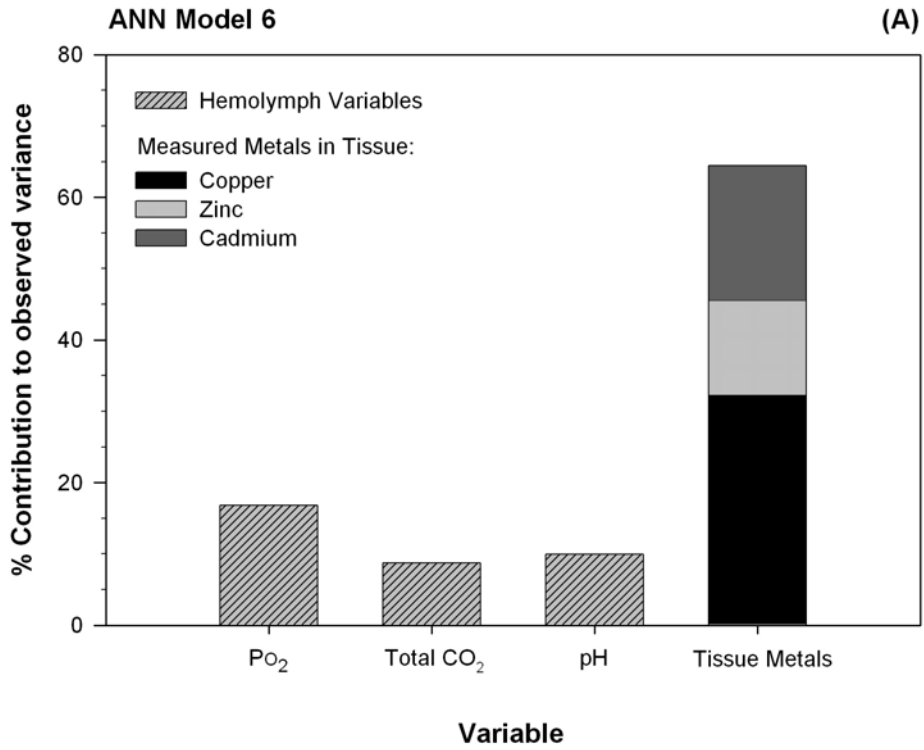
629

630 **Figure 3**
631



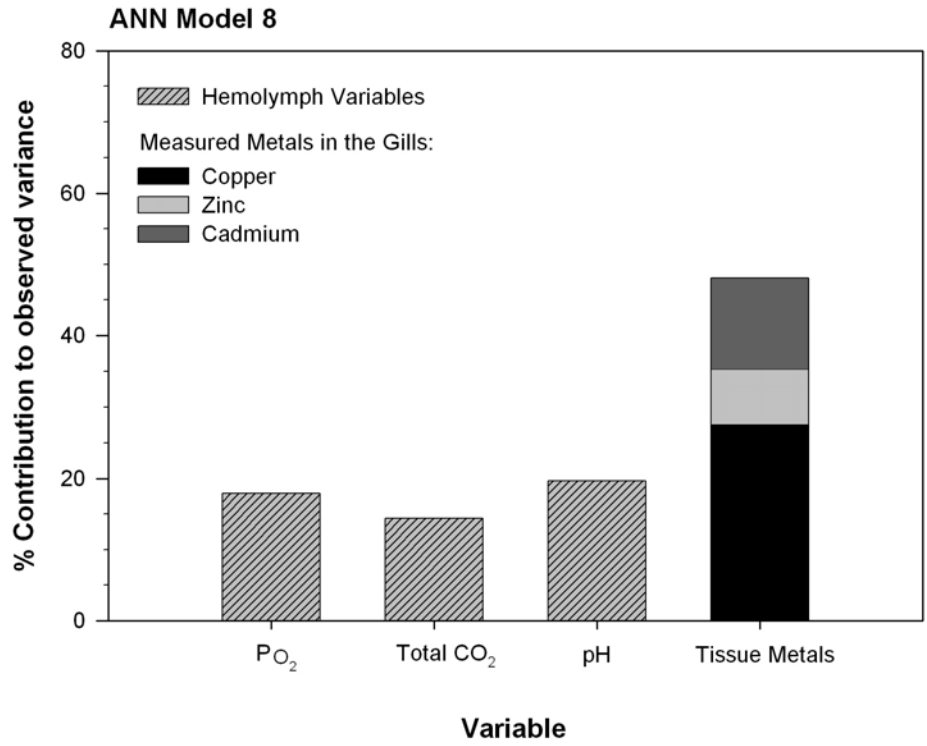
632

633 **Figure 4**
634



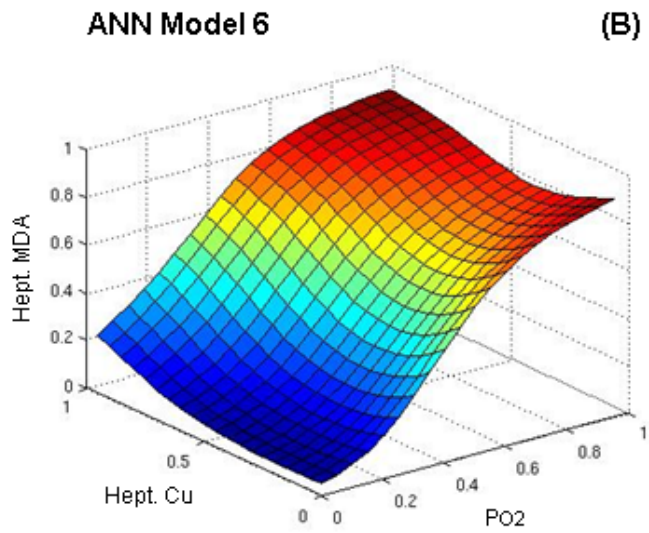
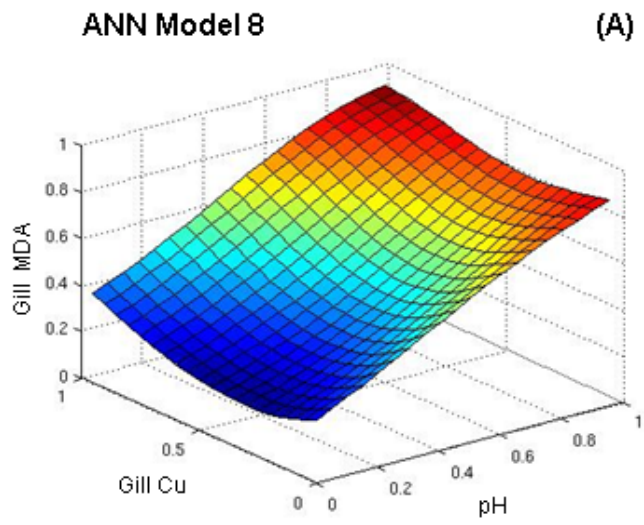
635

636 **Figure 5**



637
638

639 **Figure 6**
640
641
642



References:

- 643
644
645 Almeida, J.S., 2002. Predictive non-linear modeling of complex data by artificial neural
646 networks. *Curr. Opin. Biotechnol.* 13, 72-76.
- 647 Bishop, C. M. (1996a). Neural networks: A pattern recognition perspective. In E. Fiesler and
648 R. Beale (Eds.), *Handbook of Neural Computation*. Oxford University Press and IOP Publishing.
- 649 Bishop, C. M. (1996b). Theoretical foundations of neural networks. In P. Borchers, M. Bubak,
650 and A. Maksymowicz (Eds.), *Proceedings of Physics Computing 96, Krakow*, pp. 500–507.
651 Academic Computer Centre.
- 652 Bishop, C. M. (2006) *Pattern Recognition and Machine Learning*. Springer. New York, 738 pp.
- 653 Booth, C.E., McDonald, D.G., Walsh, P.J., 1984. Acid-base balance in the sea mussel, *Mytilus*
654 *edulis*. I. Effects of hypoxia and air-exposure on hemolymph acid-base status. *Mar. Biol. Lett.* 5,
655 347-358.
- 656 Burnett, L.E., 1988. Physiological responses to air exposure: Acid-base balance and the role of
657 branchial water stores. *Am. Zool.* 28, 125-135.
- 658 Cannon, A.J., McKendry, I.G., 2002. A graphical sensitivity analysis for statistical climate
659 models: application to Indian monsoon rainfall prediction by artificial neural networks and
660 multiple linear regression models. *Int. J. Climatol.* 22, 1687-1708.
- 661 Carpenter, D.O., Arcaro, K., Spink, D.C., 2002. Understanding the human health effects of
662 chemical mixtures. *Environ. Health Perspect.* 110, 25-42.
- 663 Chapman, R.W., Mancina, A., Beal, M. Veloso A., Rathburn, C., Blair, A., Sanger, D., Holland,
664 A.F., Warr, G.W., and DiDonato, G. (2009) A transcriptomic analysis of land use impacts on the
665 oyster, *Crassostrea virginica*, in the South Atlantic Bight. *Molecular Ecology* 18:2415-2425
- 666 Dailianis, S., Piperakis, S.M., Kaloyianni, M., 2005. Cadmium effects on ROS production and
667 DNA damage via adrenergic receptors stimulation: role of Na⁺/H⁺ exchanger and PKC. *Free*
668 *Radical Research* 39, 1059-1070.
- 669 Dankbar, D.M., Dawson, E.D., Mehlmann, M., Moore, C.L., Smagala, J.A., Shaw, M.W., Cox,
670 N.J., Kuchta, R.D., Rowlen, K.L., 2007. Diagnostic microarray for influenza B viruses. *Anal.*
671 *Chem.* 79, 2084-2090.
- 672 Dorta, D.J., Leite, S., DeMarco, K.C., Prado, I.M.R., Rodrigues, T., Mingatto, F.E., Uyemura,
673 S.A., Santos, A.C., Curti, C., 2003. A proposed sequence of events for cadmium-induced
674 mitochondrial impairment. *Journal of Inorganic Biochemistry* 97, 251-257.

675 Dovzhenko, N.V., Kurilenko, A.V., Bel'cheva, N.N., Chelomin, V.P., 2005. Cadmium-induced
676 oxidative stress in the bivalve mollusk *Modiolus modiolus*. Russ. J. Mar. Biol. 31, 309-313.

677 Elfving, T., Tedengren, M., 2002. Effects of copper on the metabolism of three species of
678 tropical oysters, *Saccostrea cucullata*, *Crassostrea lugubris* and *C. belcheri*. Aquaculture 204,
679 1157-1166.

680 Engel, D.W., 1999. Accumulation and cytosolic partitioning of metals in the American oyster
681 *Crassostrea virginica*. Mar. Environ. Res. 47, 89-102.

682 Flipič, M., Fatur, T., Vudrag, M., 2006. Molecular mechanisms of cadmium induced
683 mutagenicity. Hum. Exp. Toxicol. 25, 67-77.

684 Geret, F., Jouan, A., Turpin, V., Bebianno, M.J., Cosson, R.P., 2002a. Influence of metal
685 exposure on metallothionein synthesis and lipid peroxidation in two bivalve mollusks: the oyster
686 (*Crassostrea gigas*) and the mussel (*Mytilus edulis*). Aquat. Living Resour. 15, 61-66.

687 Geret, F., Serafim, A., Barreira, L., Bebianno, M.J., 2002b. Effect of cadmium on antioxidant
688 enzyme activities and lipid peroxidation in the gills of the clam *Ruditapes decussatus*.
689 Biomarkers 7, 242 - 256.

690 Jenny, M.J., Ringwood, A.H., Lacy, E.R., Lewitus, A.J., Kempton, J.W., Gross, P.S., Warr,
691 G.W., Chapman, R.W., 2002. Potential Indicators of stress response identified by expressed
692 sequence tag analysis of hemocytes and embryos from the American oyster, *Crassostrea*
693 *virginica*. Mar. Biotechnol. 4, 81-93.

694 Khan, J., Ringér, M., Saal, L.H., Ladanyi, M., Wesermann, F., Berthold, F., Schwab, M.,
695 Antonescu, C.R., Peterson, C., Meltzer, P.S., 2001. Classification and diagnostic prediction of
696 cancers using gene expression profiling and artificial neural networks. Nat. Med. 7, 673-679.

697 Linder, R., Dew, D., Sudhoff, H., Theegarten, D., Remberger, K., Poppl, S.J., Wagner, M., 2004.
698 The 'subsequent artificial neural network' (SANN) approach might bring more classificatory
699 power to ANN-based DNA microarray analyses. Bioinformatics 20:3544-3552.

700 Macey, B.M., Achilihu, I.O., Burnett, K., Burnett, L., 2008. Effects of hypercapnic hypoxia on
701 inactivation and elimination of *Vibrio campbellii* in the Eastern oyster, *Crassostrea virginica*.
702 Appl. Environ. Microbiol. 74, 6077-6084.

703 Marigómez, I., Soto, M., Cajaraville, M., Angulo, E., Giamberini, L., 2002. Cellular and
704 subcellular distribution of metals in molluscs. Microsc. Res. Tech. 56, 358-392.

705 Massabuau, J.-C., Tran, D., 2003. Ventilation, a recently described step limiting heavy metal
706 contamination in aquatic animals. *Journal de Physique*. IV 107, 839-843.

707 Quig, D., 1998. Cysteine metabolism and metal toxicity. *Altern. Med. Rev.* 3, 262-270.

708 Ringwood, A.H., Connors, D.E., Dinovo, A., 1998. The effects of copper exposures on cellular
709 responses in oysters. *Mar. Environ. Res.* 46, 591-595.

710 Ringwood, A.H., Connors, D.E., Keppler, C.J., Dinovo, A.A., 1999a. Biomarker studies with
711 juvenile oysters (*Crassostrea virginica*) deployed in-situ. *Biomarkers* 4, 400-414.

712 Ringwood, A.H., Connors, D.E., Keppler, C.J., Dinovo, A.A., 1999b. Biomarker studies with
713 juvenile oysters (*Crassostrea virginica*) deployed *in-situ*. *Biomarkers* 4, 400 - 414.

714 Roesijadi, G., 1996. Metallothionein and its role in toxic metal regulation. *Comp. Biochem.*
715 *Physiol. C* 113, 117-123.

716 Roméo, M., Gnassia-Barelli, M., 1997. Effect of heavy metals on lipid peroxidation in the
717 Mediterranean clam *Ruditapes decussatus*. *Comp. Biochem. Physiol. C* 118, 33-37.

718 Sanger, D.M., Holland, A.F., Scott, G.I., 1999. Tidal creek and salt marsh sediments in South
719 Carolina coastal estuaries: I. Distribution of trace metals. *Arch. Environ. Contam. Toxicol.* 37,
720 445-457.

721 Sexton, K., Hattis, D., 2007. Assessing cumulative health risks from exposure to environmental
722 mixtures - three fundamental questions. *Environ. Health Perspect.* 115, 825-832.

723 Sokolova, I.M., Ringwood, A.H., Johnson, C., 2005. Tissue-specific accumulation of cadmium
724 in subcellular compartments of eastern oysters *Crassostrea virginica* Gmelin (Bivalvia:
725 Ostreidae). *Aquat. Toxicol.* 74, 218-228.

726 Stohs, S.J., Bagchi, D., 1995a. Oxidative mechanisms in the toxicity of metal ions. *Free Radic.*
727 *Biol. Med.* 18, 321-336.

728 Stohs, S.J., Bagchi, D., 1995b. Oxidative mechanisms in the toxicity of metal ions. *Free Radical*
729 *Biology and Medicine* 18, 321-336.

730 Stohs, S.J., Bagchi, D., Hassoun, E., Bagchi, M., 2000. Oxidative mechanisms in the toxicity of
731 chromium and cadmium ions. *J. Environ. Pathol. Toxicol. Oncol.* 19, 201-213.

732 Valko, M., Morris, H., Cronin, M.T.D., 2005. Metals, Toxicity and Oxidative Stress. *Current*
733 *Medicinal Chemistry* 12, 1161-1208.

734 Viarengo, A., 1989a. Heavy metals in marine invertebrates: mechanisms of regulation and
735 toxicity at the cellular level. *Rev. Aquat. Sci.* 1, 295-317.

736 Viarengo, A., 1989b. Heavy metals in marine invertebrates: Mechanisms of regulation and
737 toxicity at the cellular level. Review in Aquatic Sciences 1, 295-317.

738 Viarengo, A., Canesi, L., Pertica, M., Poli, G., Moore, M.N., Orunesu, M., 1990. Heavy metal
739 effects on lipid peroxidation in the tissues of *Mytilus galloprovincialis* LAM. Comp. Biochem.
740 Physiol. C 97, 37-42.

741 Wang, G., Fowler, B.A., 2008. Roles of biomarkers in evaluating interactions among mixtures of
742 lead, cadmium and arsenic. Toxicol. Appl. Pharmacol. 233, 92-99.

743 Wang, Y., Fang, J., Leonard, S.S., Krishna Rao, K.M., 2004. Cadmium inhibits the electron
744 transfer chain and induces Reactive Oxygen Species. Free Radical Biology and Medicine 36,
745 1434-1443.

746 Yang, R.S.H., Dennison, J.E., 2007. Initial analyses of the relationship between "thresholds" of
747 toxicity for individual chemicals and "interaction thresholds" for chemical mixtures. Toxicol.
748 Appl. Pharmacol. 223, 133-138.

749

750